

# Synthesis and characterisation of ultrafiltration membranes functionalised with C18 as a modifier for adsorption capabilities of polyaromatic hydrocarbons

SA Mntambo<sup>1</sup>, PS Mdluli<sup>1</sup>, MM Mahlambi<sup>1</sup>, SC Onwubu<sup>1,2\*</sup> and NL Nxumalo<sup>1</sup>

<sup>1</sup>Department of Chemistry, Durban University of Technology, PO Box 1334, Durban 4000, South Africa

<sup>2</sup>Department of Dental Sciences, Durban University of Technology, PO Box 1334, Durban 4000, South Africa

## ABSTRACT

The disposal of wastewater containing polyaromatic hydrocarbons (PAHs) has been observed to be a very costly process, hence mitigation for many industrial plants continues to be a challenge. The purpose of this study was to examine the potential use of C18 as a modifier in membrane technology; thus, C18 was incorporated into poly(vinylidene fluoride) (PVDF) membranes. According to the specific composition ratios, the phase inversion process was used for dispersion of the C18 into PVDF, which was subsequently dispersed in 1-methyl-2-pyrrolidone (NMP). The resulting membranes were characterised with Fourier transform infrared spectroscopy (FTIR) and scanning electron microscopy (SEM). The mechanical properties of the membranes were analysed using dynamic mechanical analysis (DMA), whereas the thermal behaviour was studied with a thermogravimetric analyser (TGA). Furthermore, the functionality of the synthesised membrane was further evaluated by its adsorption potentials using high performance liquid chromatography equipped with an ultraviolet detector. The SEM micrographs showed successful incorporation of the C18 within the polymeric membrane (PVDF) backbone. The TGA showed that the thermal decomposition of the synthesised membranes was observed at 495 and 610°C for PVDF bare and PVDF/C18, respectively. In addition, the HPLC results obtained indicated that the C18 modified membrane was more effective in adsorbing PAHs when compared to the bare PVDF membrane. The salient features of this study therefore suggest that C18 could be used as a potential modifier for the development of PVDF membranes.

**Keywords:** PAHs, PVDF, ultra-filtration, phase inversion

## INTRODUCTION

Polyaromatic hydrocarbons (PAHs) are a class of emerging pollutants in the aquatic environment and have been a subject of discussion in recent years (Sarria-Villa et al., 2016). The presence of PAHs in the aquatic environment adversely affects marine life, as they accumulate in the digestive systems of aquatic organisms. More so, the disposal of wastewater containing PAHs has been observed to be a very costly problem to mitigate for many industrial plants (Zeledon-Toruno et al., 2007). Given the associated costs of disposing PAHs as well as its negative impact on the environment, it is important for wastewater treatment plants to find ways of removing these pollutants from wastewater before disposal to the environment.

In recent decades, membrane technology has been effectively used in the water treatment industry due to its competence in terms of its chemical structure and stability, hydrophobicity, hydrophilicity, permeability (high and low perm-selectivity), low energy consumption, and mechanical as well as thermal resistance (Fan et al., 2008; Rajesh et al., 2013). At present, almost all membranes used for industrial processes are made from inorganic materials and/or organic polymers, and the latter dominates the existing membrane market. Examples of organic polymers used for membrane synthesis include polysulfone (PSF) (Chen et al., 1996), poly(ether sulfone) (PES) (Idris et al., 2007), poly-acrylonitrile (PAN), polyamide, polyimide (Huang et al., 2006; Wang et al., 2009), poly(vinylidene fluoride) (PVDF) (Mahlambi et al., 2014; Yan

et al., 2005) and polytetrafluoroethylene (PTFE) (Grevstad and Leknes, 1993).

Among the aforementioned polymers, PVDF is one of the most widely used membrane material and has been paid much attention by researchers and manufacturers in recent years. Furthermore, Ma et al. (2017) and Shen et al. (2017) have reported that the PVDF membrane is essential, as it directly affects process efficiency and practical application value, and further suggested that this may be the result of its semi-crystalline polymeric material with repeated unit of  $-(\text{CH}_2\text{CF}_2)_n-$  (Zhu et al. 2014).

So far, there have been quite a number of studies done on the application fields of PVDF membranes, including microfiltration (MF), ultrafiltration (UF), membrane bioreactor (MBR), membrane distillation, gas separation and stripping, as well as removal of PAHs from water (Kang and Cao, 2014). Although PVDF polymers are commonly used in wastewater treatment plants, Rana and Matsuura (2010) noted that PVDF membranes are susceptible to fouling while treating aqueous solutions containing natural organic matter, e.g. proteins, which are easily adsorbed onto the membrane surface or block the surface pores. Modifying PVDF is therefore critical if it is to be effectively used for the removal of PAHs in wastewater.

Phase inversion is a chemical phenomenon exploited in the fabrication of artificial membranes (Baker, 2000; Hester et al., 1999). It is performed by removing the solvent from a liquid-polymer solution, leaving a porous, solid membrane. Phase inversion is basically a process of controlled polymer transformation from a liquid phase to a solid phase or a polymeric state (Kimmerle and Strathmann, 1990). There are four basic techniques used to create phase inversion membranes: precipitation from vapour phase, precipitation by controlled evaporation, thermally induced phase separation,

\* To whom all correspondence should be addressed.  
e-mail: [profstan4christ@yahoo.com](mailto:profstan4christ@yahoo.com)

Received 19 January 2018, accepted in revised form 28 November 2018.

and immersion precipitation. Out of the four, immersion precipitation was chosen to best suit the study due to its simplicity for preparing polymeric membranes. Fig. 1 illustrates the technique.

Several studies have indicated that modifiers such as C18 (Alsaiee et al., 2016), charcoal (Pradeep et al., 2016), molecularly imprinted polymers (MIPs) (Altintas et al. 2016), and carbon nanotubes (CNTs) (Chen et al., 2016) can alter the hydrophilicity of PVDF polymeric material. It is generally accepted that an increase in hydrophilicity offers better membrane fouling resistance (Kang and Cao, 2012; Rana and Matsuura, 2010; Saljoughi and Mousavi, 2012).

This paper reports on the use of C18 in modifying PVDF for the adsorption of PAHs from water, and is mainly focused on the affected areas of the south coast of Durban. These sites are of concern due to remediation and new industrial erections that took place in the early 2000s. Hence, sampling is focused on the south coast region. It has been demonstrated that C18 is highly promissory in wastewater treatment, not only because of the high specificity of the active sites but also due to the high purity separations it brings to water purification technology (Han et al., 2017). Hence preparing a membrane infused with C18 will likely enhance the performance of the PVDF polymeric membrane, especially in aqueous solutions which is also crucial for in-vivo applications. To this end, no reports exist in literature on the modification of PVDF using C18 for PAH removal in water. This work reports on the successful synthesis of PVDF membranes functionalised (or incorporated) with C18 modifier as well as their adsorption capabilities for PAHs from wastewater.

## METHODS

All materials were obtained from suppliers and used without any further purification. 1-methyl-2-pyrrolidone (NMP) (85 wt %) and poly (vinylidene fluoride) pellets (PVDF) (97%) were obtained from Sigma Aldrich, South Africa. C18 SPE (500 mg/6 mL) cartridges were obtained from Separations, South Africa. The mixture of the casting solution was mixed according to the composition ratio presented by Table 1. Pyrene, fluorene and anthracene powders were also obtained from Sigma Aldrich, South Africa. High performance liquid chromatography (HPLC) grade acetonitrile (99.9%), acetone (99.9%), toluene (99.9%) and methanol (99.9%) were obtained from Merck group and were used as obtained without further purification. Formic acid and sodium hydroxide were also obtained Sigma Aldrich, South Africa. Double deionised water was obtained using the Perfect Water purification system. The polymer solutions were cast on a clean glass using a manual

Membrane	PVDF (wt. %)	C18 (wt. %)	NMP (wt. %)
PVDF bare	17.00	0.0	83.00
0.1 %PVDF/C18	16.98	0.017	83.00
0.2 % PVDF/C18	16.97	0.034	83.00
0.3 % PVDF/C18	16.95	0.051	83.00

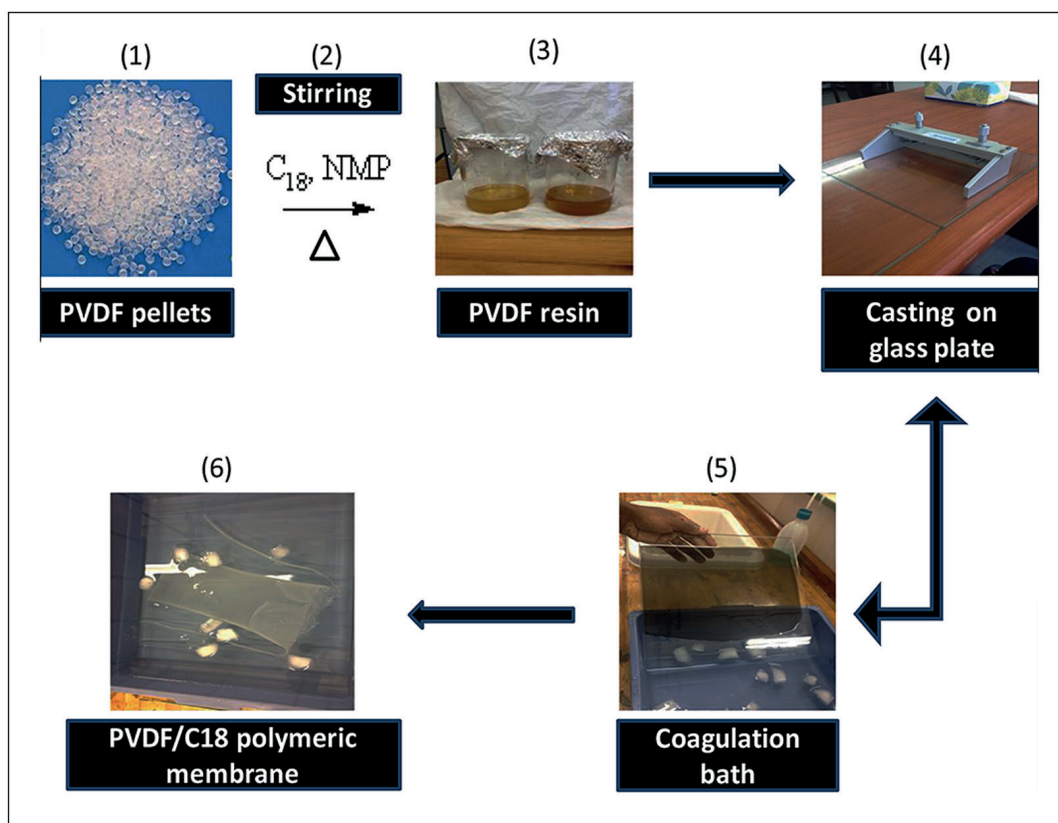


Figure 1

The graphical representation of the preparation process of PVDF/C18 polymeric membrane by phase inversion

technique with a stainless-steel casting knife sourced from Lasec (Johannesburg, South Africa).

### Instrumentation

A dynamic mechanical analysis (DMA) Q800 TA technique was used to study the viscoelastic behaviour of both the pure and modified membranes. For analysis purposes, a sinusoidal stress was applied and the strain in the material was measured which allowed for the determination of the complex modulus. The temperature of the sample or the frequency of the stress were often varied, leading to variations in the complex modulus. This approach was used to locate the glass transition temperature of the material, as well as to identify transitions corresponding to other molecular motions. A TGA 2050 thermo-gravimetric analyser was used to determine the thermal properties of the pristine PVDF and the mixed matrix membranes. For analyses, the samples were heated up to 600°C at a heating rate of 10°C/min under a dry nitrogen atmosphere. An infra-red Tensor II Bruker Optics spectroscopy (IR) analysis was used to examine and study the functional groups on the membrane surfaces of both the pristine and C18-infused PVDF mixed matrix membranes. All spectra were collected between 350 and 4 000 cm<sup>-1</sup>. The surface morphology of the pristine PVDF and C18/PVDF membranes were studied using a Hitachi S-4300 scanning electron microscope (SEM). The samples were mounted on the sample studs and a thin layer of gold was sputtered on the sample surface for imaging purpose. The SEM measurements were performed at an accelerating voltage of 10 kV and at different magnifications.

### Synthesis of PVDF membranes

The phase inversion process was used for the synthesis of the membranes. The C18 and the PVDF were dispersed in 1-methyl-2-pyrrolidone (NMP) solution according to the specific composition ratios. The mass of the modifier was varied to observe and monitor adsorption techniques for different membrane compositions. The polymeric mixture was then stirred and allowed to mix for 8 h at 45°C and allowed to settle for 2 h. This solution was then cast onto a clean glass plate. A casting knife with an adjustable blade height set to a maximum of 150 µm was used. After casting, the glass plate was immediately immersed in a coagulation bath containing ice-deionised water for a period of 10 min. The resultant membranes were further rinsed 3 times with deionised water before being stored in a refrigerator (at 4°C) in water bags with deionised water before usage.

### Immersion precipitation

Phase inversion via immersion precipitation is the most widely-used membrane preparation method. As seen in Fig. 1, after continuous stirring (2) of the polymer (1) and solvent (NMP) they form the casting solution (3) which is cast onto a clean glass plate (4) and then submerged in a coagulation bath (5). Due to the solvent and nonsolvent exchange, precipitation takes place and a polymeric membrane (6) is formed. The combination of phase separation and mass transfer affects the membrane structure.

### Water content percentage of PVDF membranes

For the evaluation of the pure water flux of the prepared ultrafiltration membranes, water content percentage was measured. To conduct this experiment, a certain weight of membrane pieces was immersed in distilled water for about 24 h. Secondly, the wet membranes were immediately placed between two dry paper sheets to remove additional drops of water on the surface and then weighed immediately. After that, they were placed in an oven at a fixed temperature (50°C) for another 24 h and weighed. Water content percentage was measured as the weight difference between dried and wet membranes. The water content percentage was calculated using the equation reported by Bagheripour et al. (2016) and James (1999):

$$\text{Water content (\%)} = \frac{W_w - W_d}{W_w} \times 100 \% \quad (1)$$

Where  $W_w$  and  $W_d$  are the wet and dried membrane weight, respectively. Measurements were taken 3 times, and average values were reported to minimise errors. Moreover, the results obtained from the above formulation can be used for overall porosity determination (using gravimetric method), as declared in the equation:

$$\text{Porosity (\%)} = \frac{W_w - W_d}{\rho_f V_m} \times 100 \% \quad (2)$$

where  $\rho_f$  represents the density of water (g/cm<sup>3</sup>) and  $V_m$  represents the membrane volume (cm<sup>3</sup>) (Vatanpour et al., 2012). All experiments were also performed in triplicate and the average values recorded as results to mitigate possible experimental errors.

## RESULTS AND DISCUSSION

### Characterization of membranes

#### Scanning electron microscopy (SEM)

SEM analysis was used to study the morphological changes in the membranes as the particles of C18 were infused within the PVDF polymer backbone. Comparison of the surface pore structure (Fig. 2) of the PVDF bare and PVDF/C18 membrane revealed that a surface section of all C18 modified membranes featured a rougher surface region. These rough surfaces were less prevalent in pristine PVDF membranes and they were characterised by a highly dense surface morphology section with few macro voids also observed on the surface.

The SEM micrograph of the C18 modified PVDF membrane (PVDF/C18) (Fig. 2b) visibly showed the incorporation of the modifier within the polymeric membrane (PVDF). Moreover, a less porous structure was observed in the modified membrane. In contrast, and as shown in Fig. 2a, more noticeable and bigger pores were observed for the pristine membrane. The white pigment observed on the surface of the PVDF/C18 was consistent with results by Guo-Dong Kang (2014) and could be attributed to the dispersion of C18 on the surface of the polymer. Furthermore, the dispersion of C18 on the membrane appears to be clogging the pores of the PVDF membranes. This, according to Petersen and Cadotte (1990), allows a specific surface permeability, which in turn entraps the selected pollutants.

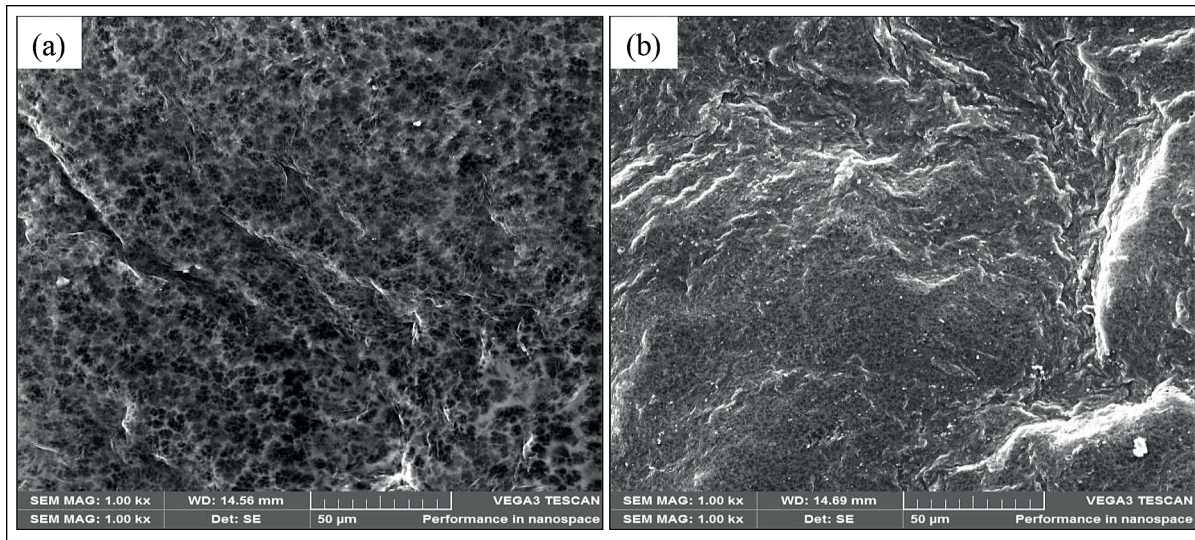


**Figure 2**  
SEM micrographs: (a) PVDF membrane and (b) PVDF/C18 membrane

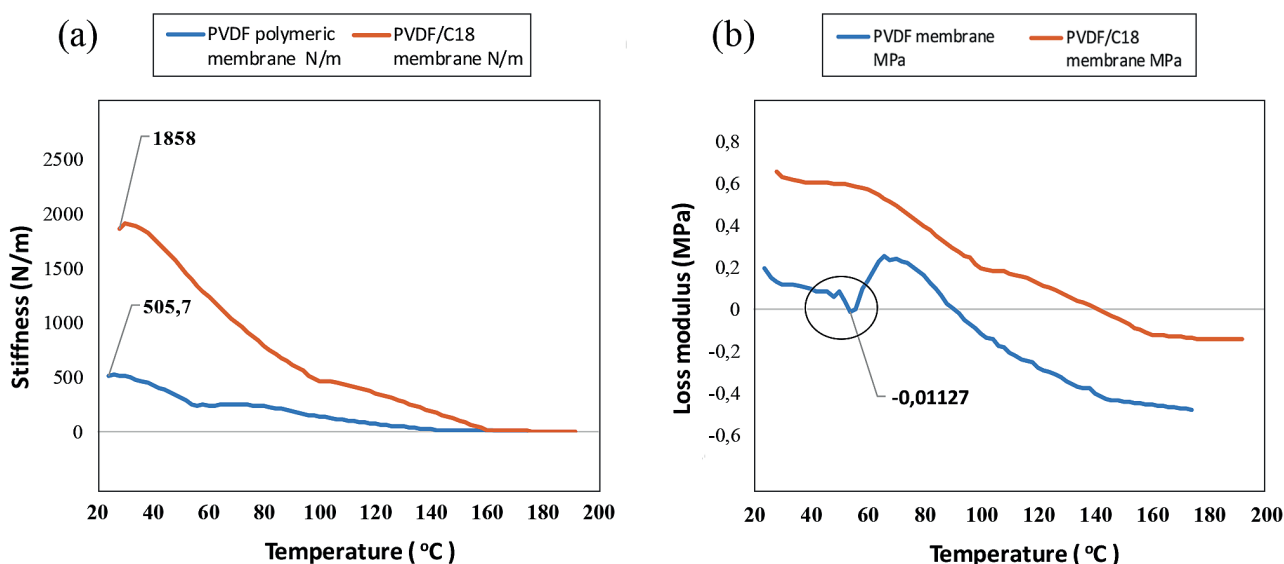


**Figure 3**  
(a) Stiffness of PVDF membrane vs PVDF/C18; (b) loss modulus of PVDF membrane vs PVDF/C18

### Dynamic mechanical analysis (DMA)

The mechanical behaviour, such as the stiffness and loss modulus, of the PVDF membrane before and after addition of C18 was studied using DMA. According to Yang et al. (2007), the modification of PVDF membrane with an inorganic or organic additive tends to have an observable effect on the polymeric membrane. As shown in Fig. 3a, net differences were observed in stiffness properties between the PVDF membrane and PVDF/C18 polymer. For example, the addition of C18 to the PVDF membrane increased its stiffness properties from 505.7 to 1 858 N/m. This change in the stiffness properties of PVDF after modification with C18 could be attributed to the change in the C—C bond energy (Padaki, 2012).

Equally significant, the graphical presentation of the loss modulus (Fig. 3b) showed observable differences between the PVDF and PVDF/C18 polymeric membrane. Liu et al. (2011) previously reported that the PVDF membranes have a thermal decomposition temperature of virtually 316°C. Contrary to this, and as shown in Fig. 3b, the PVDF completely degraded at 200°C. This difference could be attributed to the molecular weight of PVDF pellets employed in this study. In addition, and as seen by the degradation curve, the membrane performs a rare degradation caused by the C—F bond when it burns at 60°C. In contrast, the addition of C18 to the PVDF improved the stability of the material, as no degradation was visible at 60°C after infusion with C18.

### Thermogravimetric analysis (TGA)

The TGA graph for the pristine PVDF and the PVDF/C18 mixed matrix membranes was studied for a temperature range of 0–950°C and is displayed in Fig. 4. As seen in Fig. 4a, the single thermal event observed at 450°C was attributed to the decomposition of the PVDF membrane (Li et al., 2012). In contrast, Fig. 4b revealed a decomposition temperature beyond 500°C; hence it can be inferred that the incorporation of C18 improved the thermal stability of PVDF membranes. This graph further displays the combustion of moisture at 100°C and this can be attributed to the C18 chain which consists of a long chain with moisture.

Figure 4 showed that the parent polymer (PVDF) exhibited only about 5% weight loss at the beginning of the heating run. This agrees with the study done by Bagheripour et al. (2016) and is due to the elastic nature of the PVDF material. Furthermore, the thermal degradation process displayed by the bare PVDF membrane (Fig. 4a) showed that it was completely degraded below 500°C. In contrast, the final thermal heat of the PVDF membrane (Fig. 4a) from 500–800°C took place uniformly, which is indicative of the organic nature of the polymer. From Fig. 4b, it is seen that the PVDF/C18 membrane follows a different pattern, in which the last thermal event takes place when there is about 20% mass remaining. This indicates the successful incorporation of C18 since it loses more weight that is given by the long carbonyl polymeric chain of C18 on the PVDF cavities.

### Attenuated total reflectance Fourier transform infrared (ATR-FTIR)

An FTIR equipped with an attenuated total reflectance (ATR) accessory that permits direct measurement of samples with no sample preparation was used. Firstly, the raw material, i.e. (PVDF pellets), was studied separately. The PVDF pellets, which make up about 50% of the membrane, were used as a reference point to study the intensity and functional groups of the ATR scans (Fig. 5a). Every peak that appeared on the PVDF pellets was observed in every scan to signal its presence. The suit in which the PVDF membranes were cast was further indicated by the common C—H stretch around 3 250 cm<sup>-1</sup>; however, the dissimilarity observed was identified by the peak intensity, shape and position, which are the basis of the ATR-FTIR spectroscopy (Ficai et al., 2010).

#### Peak intensity

The C-H stretch on the pristine PVDF membrane showed a small peak, in terms of height (Fig. 6a), which absorbed at an intensity of 82.55% transmittance, compared to that of the PVDF/C18 mixed matrix membrane (Fig. 6b) which absorbed at an intensity of 65.56% transmittance. At around 1 200 cm<sup>-1</sup>, the spectra show the presence of the C—F functional group and these specific peaks appear in all membranes and they are attributed to the  $-(CH_2-CF_2)_n-$  in the PVDF polymer. Figure 6c shows the presence of a C=C stretch at 1 600 cm<sup>-1</sup> which is indicative of an alkene that is formed, and at 1 720 cm<sup>-1</sup> a C=O (carbonyl) peak was observed.

The FTIR spectra fingerprint region, vibrations, stretching and fingerprint region are presented in detail in Table 3.

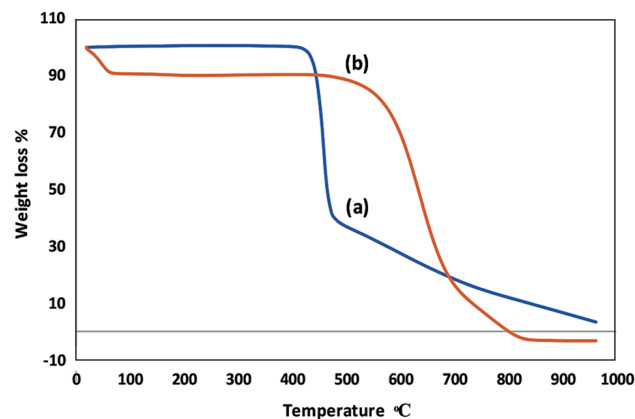


**Figure 4**  
Thermograms of (a) PVDF membrane and (b) PVDF/C18 membrane

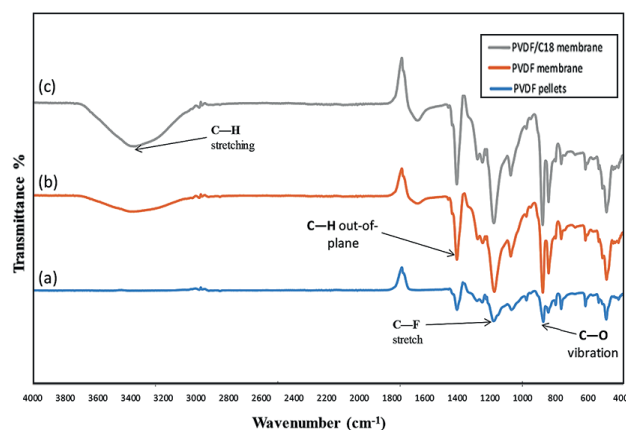


**Figure 5**  
The FTIR spectra of (a) PVDF pellets; (b) PVDF membrane; (c) PVDF/C18 membrane

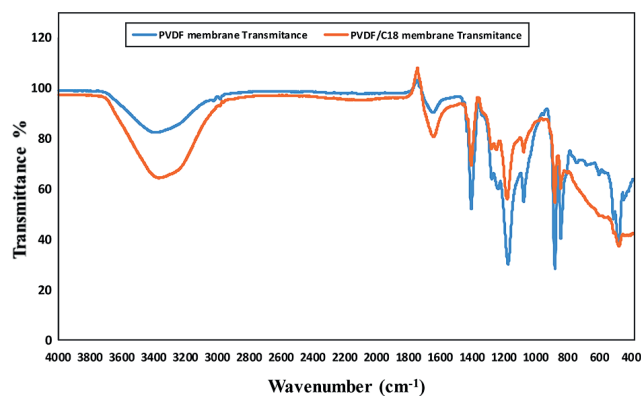


**Figure 6**  
The peak height of (a) PVDF membrane (b) PVDF/C18 membrane

Membrane type	Temperature (°C)	Weight loss (%)
(a) PVDF membrane (bare)	492	23.19
(b) PVDF/C18 membrane	610	55.43

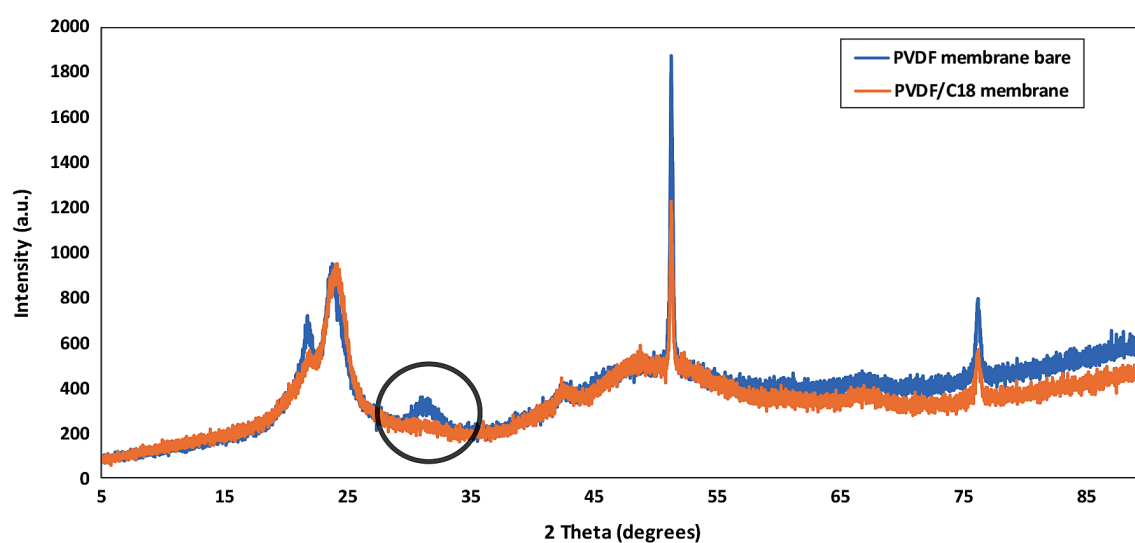
\*\*The values were obtained from the TGA analysis software

TABLE 3 The spectral ranges based on peak presence in the ATR scan				
NMP	PVDF	C18	Polymeric membrane wavenumbers	Functional groups and vibrational mode
680 cm <sup>-1</sup>	–	–	680 cm <sup>-1</sup>	The C=O ring bending
680 cm <sup>-1</sup>	–	–	680 cm <sup>-1</sup>	C–H out-of-plan vibrations between 650 and 1 000 cm <sup>-1</sup>
799 cm <sup>-1</sup>	769 cm <sup>-1</sup> 805 cm <sup>-1</sup>	780 cm <sup>-1</sup>	785 cm <sup>-1</sup> 815 cm <sup>-1</sup>	
<b>Bending</b>				
–	860 cm <sup>-1</sup>	–	859 cm <sup>-1</sup>	CH <sub>2</sub> rocking
780 cm <sup>-1</sup>	–	850 cm <sup>-1</sup>	855 cm <sup>-1</sup>	C–H out-of-plane deformation
955 cm <sup>-1</sup>	932 cm <sup>-1</sup> 1 040 cm <sup>-1</sup>	1 050 cm <sup>-1</sup>	932 cm <sup>-1</sup> 1 037 cm <sup>-1</sup>	C–C backbone vibration (weak) stretching
1 100 cm <sup>-1</sup>	–	–	1 037 cm <sup>-1</sup>	C–O vibration stretching C–F out-of-plane deformation
–	1 230 cm <sup>-1</sup>	–	1 225 cm <sup>-1</sup> 1 230 cm <sup>-1</sup>	
–	1 219 cm <sup>-1</sup>	–	1 219 cm <sup>-1</sup>	C–F stretch
1 300 cm <sup>-1</sup>	–	–	1 372 cm <sup>-1</sup>	Interaction of O–H and C–O stretching in C–O–H
<b>Bending, stretching</b>				
1 488 cm <sup>-1</sup>	–	1 488 cm <sup>-1</sup>	1 443 cm <sup>-1</sup> 1 500 cm <sup>-1</sup>	C=C vibration, stretching, CH <sub>2</sub> (C–H bond) vibration, bending
–	1 477 cm <sup>-1</sup>	1 477 cm <sup>-1</sup>	1 546 cm <sup>-1</sup>	C–H out-of-plane deformation C=C vibrations (weak) and unknown vibrations from fingerprinting
–	–	–	1 600 cm <sup>-1</sup>	
2 998 cm <sup>-1</sup>	3 240 cm <sup>-1</sup>	2 990 cm <sup>-1</sup>	2 882 cm <sup>-1</sup> 2 948 cm <sup>-1</sup>	Asymmetric vibrations of C–H bonds of methyl groups C–H stretching
3 001 cm <sup>-1</sup>	3 001 cm <sup>-1</sup>	2 990 cm <sup>-1</sup>	3 250 cm <sup>-1</sup>	

### X-ray diffraction (XRD)

The diffractograms shown in Fig. 7 agree with Bragg's law. According to Bragg's law of diffraction, no peak is observed unless the condition for constructive interference ( $\delta = n\lambda$ , with  $n$  an integer) is precisely met, which further describes the condition on  $\theta$  for the constructive interference to be at

its strongest (Meyers and Myers, 1997). After XRD analysis of the membranes was performed, PVDF displayed a common tendency to crystallise in 4 different polymorphs  $\alpha$ ,  $\beta$ ,  $\gamma$  and  $\delta$ , and each crystal structure displays various polymorphs (Kim et al., 2002). Figure 7 further shows the XRD patterns of PVDF membranes with and without the additive (C18). The diffraction peaks at  $2\theta = 21.8$  and  $23.6$  degrees were assigned to



**Figure 7**  
XRD graphs of PVDF membrane bare and PVDF/C18 membrane

$\alpha$  (010) and  $\alpha$  (110), respectively, and these were characteristic of the  $\alpha$ -phase crystal structure (Kim et al., 2002). After the addition of C18, it was observed that the peak at  $2\theta = 28.2^\circ$  ( $\beta$  110) had disappeared. The disappearance of this peak is an indication that there is some chemical interaction between the C18 and PVDF polymer backbone.

Moreover, the peak intensity of the PVDF/C18 membrane at  $2\theta 28.2^\circ$  (indicated by circle in Fig. 7) appear reduced and this may be attributed to the decrease in PVDF transparency caused by the micro-sized C18 particle aggregation. As a result, the electronic field in the additive changed and this led to a change in the relative intensity of the modified polymeric membrane. PVDF polymer and C18 particles are known to possess low compatibility, and each material has its own crystal regions in the blended membranes; this was also shown by the fact that the samples essentially maintain their crystal configuration throughout modification (Zhang et al., 2009).

### Water content and porosity percentage

These two parameters were studied to confirm whether incorporation of C18 influenced the hydrophilicity/hydrophobicity properties of the PVDF membranes. From the results obtained (Fig. 8), the membrane water content gradually increased with increase in C18 concentration. This further indicates that a more hydrophilic membrane was produced by the increase of C18 percentage in the casting solution. This may be influenced by the hydrophilic characteristic of C18, as this modifier is said to belong to the non-polar family group (Deng et al., 2010; Shen et al., 2012). The existence of  $CF_2$  on the PVDF polymeric membrane with its electronegative nature highly influences the strong hydrophilic group on the C18 surface to result in a more hydrophilic polymeric membrane after blending into the prepared casting solution (Loh and Wang, 2012). Moreover, this phenomenon results in an increase in cavities or void size and number in the prepared polymeric membranes, resulting in more space for water adsorption and accumulation; hence, water content and porosity increases on the membrane. Similar trends have been observed for SPES infused in PVDF membranes (Rahimpour 2010).

Figure 9 expresses the calculated porosity of prepared membranes against % C18 used to fabricate the membrane.

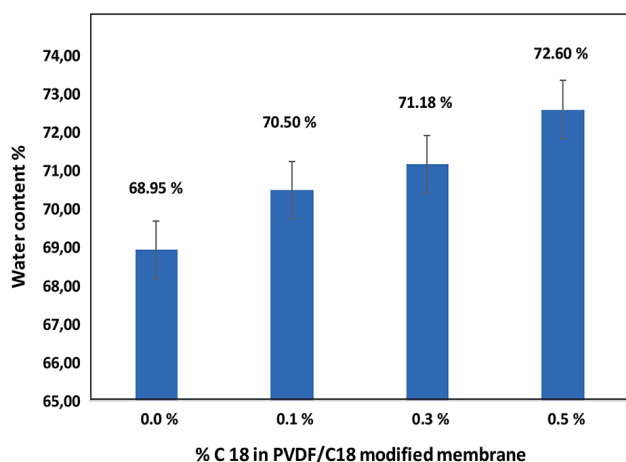


Figure 8

Effects on polymer binder blend ration on membrane water content %

The results obtained also revealed that increasing the C18 concentration resulted in increased porosity in the membrane matrix, with reference to pristine PVDF membranes (Gardner, 1965). The results are in good agreement with Fig. 1a and Fig. 1b (SEM images). The membrane manufactured by various C18 % concentrations signalled the formation of spherical macro-voids in the structure. Increasing C18 % in the casting solution gave rise to greater porosity in membrane structure – this also led to an increased number of macro-voids and a spongy structure which is responsible for the increase in the hydrophilicity of the casting solution and its effect on phase inversion occurrence (Blanco, 2006).

### Quantification of PAHs with high performance liquid chromatography (HPLC)

Pyrene, fluorene and anthracene were used to study the absorptive capabilities of the synthesised membranes. High performance liquid chromatography (HPLC) was used to determine the recoveries, limit of detection and limits of quantification in this study. An HPLC that consists of a Waters 600E pump, UV/vis and fluorescence detectors was employed. Samples and standards were injected using a syringe 7010 injector equipped with a 20  $\mu$ L loop. Compounds were separated using a Gemini  $C_{18}$  HPLC column (150 x 4.60 mm x 5  $\mu$ m). Shimadzu LC Solutions software was used for recording of chromatograms and data collection. UV/vis detector settings were set at 252 nm for PAHs.

HPLC condition	Designation or value
Pmax	3 000 psi
Pmin	0
Column	Gemini 5 $\mu$ C18 110A,length150x4.60 mm, ID 5 $\mu$
Mobile phase	Acetonitrile/Water (80/20)
Detector wavelength	UV-252 nm
Flow rate	1.0 mL/min

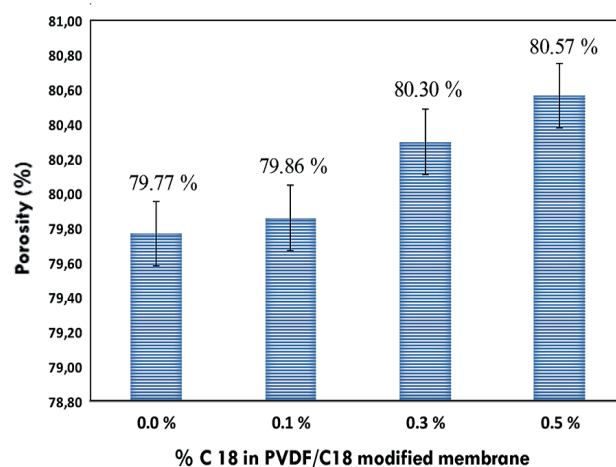
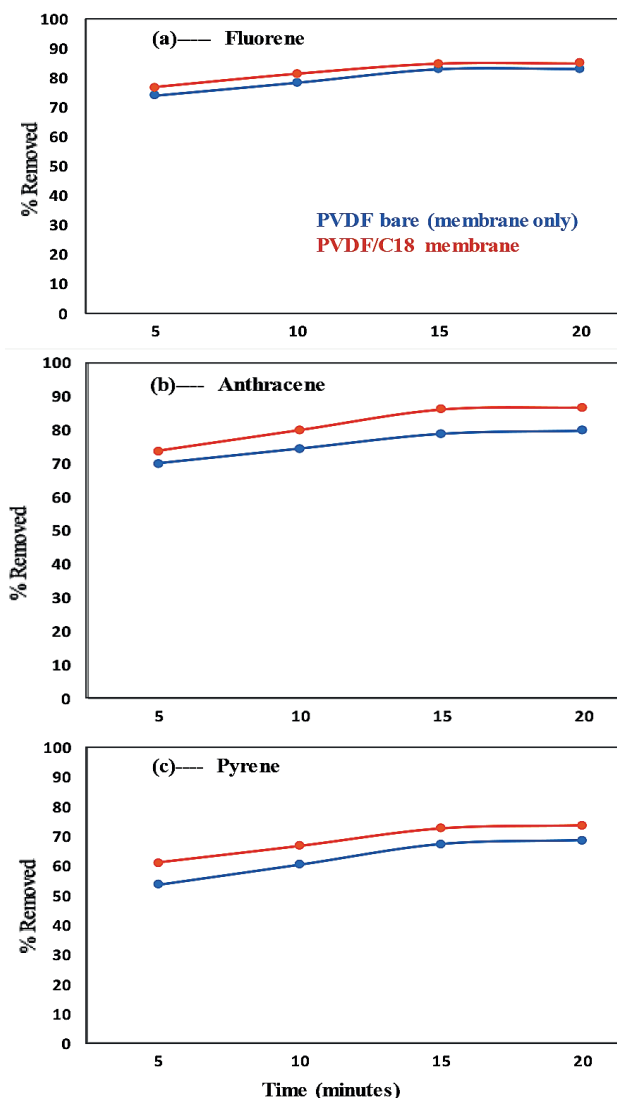


Figure 9

Effects of polymer binder blend ratios on membrane porosity (%)

### Effect of contact time

For determination of the effect of contact time on the adsorption of the PAHs by the membranes, the % removed as a function of time was used while keeping constant the sample pH, initial concentration, adsorbent mass (50 mg) and sample volume (10 mL) (Panahi et al. 2013). The results presented in Fig. 10 show that maximum adsorption was achieved in 15 min, where the extraction efficiency was better than 65% and 75% for all compounds adsorbed onto the PVDF and PVDF/C18 polymeric membrane, respectively. After 15 min, the slope of % PAH removed vs time was observed to be 0, which indicated that no significant adsorption took place beyond that time interval (Fig. 10a, b and c). However, the evaluation was carried out until 20 min had passed and this showed a similar adsorption capability beyond the 15-min time scale for both the pristine PVDF and PVDF/C18 membranes. These results therefore confirm that equilibrium was reached during the first 15 min, starting from the moment of exposure of PVDF/C18 to the solution; after equilibrium, no adsorption was observed



**Figure 10**

% PAH removal vs time interval: (a) fluorene, (b) anthracene, and (c) pyrene

(Idris et al., 2007). However, fluorene (Fig. 10a) displayed better adsorption compared to anthracene (Fig. 10b) and pyrene (Fig. 10c). Pyrene had the worst adsorption relative to the other PAHs and this is largely due to the polarities of these PAHs. Furthermore, to ensure maximum uptake of target pollutants from the aqueous samples, a contact time of 15 min was used in succeeding experiments. Overall, a better % removal was observed for PVDF/C18 membrane compared to PVDF bare and this was observed for all analysed PAHs (Fig. 10 a, b, c).

The main aim of this study was to compare the adsorption and recoveries of PAHs between pristine PVDF membrane (membrane without C18) and PVDF/C18 membrane, using liquid chromatography. The peak intensities displayed in Fig. 11a–c, further explain the constant removal of PAHs in the sample within the same optimum contact time (15 min), since the bar graphs show no significant change after 15 min in contact with the membrane. The data represented in Fig. 11 indicate that the retention times of the PAHs were influenced by the polarity, electronegativity and molecular structure of the PAHs (Sicilia et al. 1999). Hence the order of elution was, fluorene (2.83 min), anthracene (3.72 min) and pyrene (4.08min)

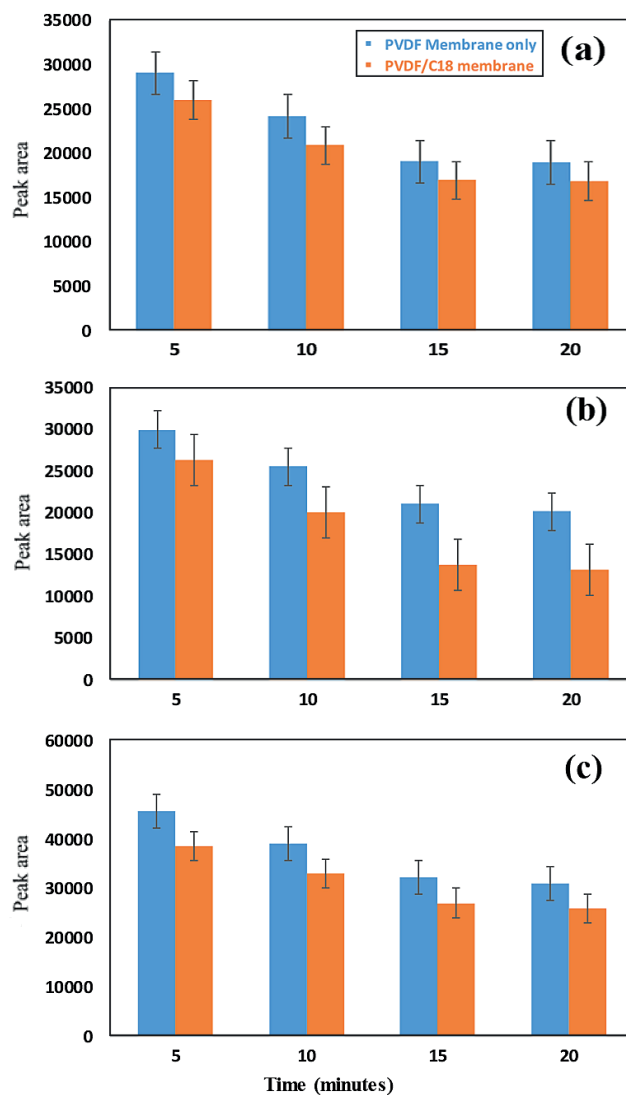


**Figure 11**

Peak area vs time interval of: (a) fluorene; (b) anthracene; (c) pyrene

## CONCLUSIONS

The pristine PVDF membranes and the PVDF/C18 membranes were successfully produced via the phase inversion method and characterised with conventional techniques. Polyaromatic hydrocarbons have been of concern for aquatic organisms and humans. In this study, the measured concentrations were within the legal limits of the South African Department of Water and Sanitation.

The significance of incorporation of C18 into PVDF-pristine was further displayed by different spectra, thermal stability and degradation when the two membranes were evaluated. Also, incorporating C18 into the PVDF membrane was found to enhance the adsorptive capabilities of the membranes. It was also found that the modification of hydrophobic PVDF membrane with C18 improved the hydrophilicity of the PVDF membrane. From studies of the surface morphology, water content, porosity percentage and FTIR results, it can be concluded that the C18 was deposited onto the membrane surfaces and in the pores and improved the performance of the polymer. The hydrophilicity of the modified membrane increased with increasing C18 concentration; hence, the modification method significantly affected the deposition of C18 on the membrane surface and the walls of the pores. The PVDF/C18 mixed matrix membranes were also found to have improved PAH adsorptive capabilities compared to the pristine PVDF membranes; thus the incorporation of the C18 improved the performance of the membrane.

It may be beneficial to replicate the conducted experiment in another area, which has higher PAH concentrations in wastewater or water bodies. This could allow the study of the PVDF/C18 membranes to be performed at an industrial scale.

## REFERENCES

- ALSBAIEE A, SMITH BJ, XIAO L, LING Y, HELBLING DE and DICHTEL WR (2016) Rapid removal of organic micropollutants from water by a porous  $\beta$ -cyclodextrin polymer. *Nature* **529** (7585) 190–194. <https://doi.org/10.1038/nature16185>
- ALTINTAS Z, CHIANELLA I, DA PONTE G, PAULUSSEN S, GAETA S and TOTHILL IE (2016) Development of functionalized nanostructured polymeric membranes for water purification. *Chem. Eng. J.* **300** 358–366. <https://doi.org/10.1016/j.cej.2016.04.121>
- BAGHERIPOUR E, MOGHADASSI A and HOSSEINI S (2016) Preparation and characterization of PES-blend-sulfonated PVC nanofiltration membranes: Investigation of polymers blend ratio. *Arab. J. Sci. Eng.* **7** (41) 2545–2552. <https://doi.org/10.1007/s13369-016-2026-5>
- BAKER R (2000) *Membrane Technology*. Wiley Online Library.
- BLANCO JFS, NGUYEN QT and SCHAETZEL P (2006) Formation and morphology studies of different polysulfone-based membranes made by wet phase inversion process. *J. Membrane Sci.* **283** 27. <https://doi.org/10.1016/j.memsci.2006.06.011>
- CHEN MH, CHIAO TC and TSENG TW (1996) Preparation of sulfonated polysulfone/polysulfone and aminated polysulfone/polysulfone blend membranes. *J. Appl. Polym. Sci.* **61** (7) 1205–1209. [https://doi.org/10.1002/\(SICI\)1097-4628\(19960815\)61:7<1205::AID-APP16>3.0.CO;2-W](https://doi.org/10.1002/(SICI)1097-4628(19960815)61:7<1205::AID-APP16>3.0.CO;2-W)
- CHEN X, QIU M, DING H, FU K and FAN Y (2016) A reduced graphene oxide nanofiltration membrane intercalated by well-dispersed carbon nanotubes for drinking water purification. *Nanoscale* **8** (10) 5696–5705. <https://doi.org/10.1039/C5NR08697C>
- DENG B, YU M, YANG X, ZHANG B, LI L, XIE L, LI J and LU X (2010) Antifouling microfiltration membranes prepared from acrylic acid or methacrylic acid grafted poly (vinylidene fluoride) powder synthesized via pre-irradiation induced graft polymerization. *J. Membrane Sci.* **350** (1–2) 252–258. <https://doi.org/10.1016/j.memsci.2009.12.035>
- FAN Z, WANG Z, SUN N, WANG J and WANG S (2008) Performance improvement of polysulfone ultrafiltration membrane by blending with polyaniline nanofibers. *J. Membrane Sci.* **320** (1) 363–371. <https://doi.org/10.1016/j.memsci.2008.04.019>
- FICAI D, FICAI A, VOICU G, VASILE BS, GURAN C and ANDRONESCU E (2010) Polysulfone based membranes with desired pores characteristics. *Mater. Plastice* **47** (1) 24–27.
- GARDNER WH (1965) Water content. In: Black CA (ed.) *Methods of Soil Analysis. Part 1. Physical and Mineralogical Properties, including Statistics of Measurement and Sampling*. American Society of Agronomy, Madison. 82–127.
- GREVSTAD HJ and LEKNES KN (1993) Ultrastructure of plaque associated with polytetrafluoroethylene (PTFE) membranes used for guided tissue regeneration. *J. Clin. Periodontol.* **20** (3) 193–198. <https://doi.org/10.1111/j.1600-051X.1993.tb00343.x>
- GUO-DONG KANG Y-MC (2014) Application and modification of poly(vinylidene fluoride) (PVDF) membranes – A review. *J. Membrane Sci.* **463** 145–165. <https://doi.org/10.1016/j.memsci.2014.03.055>
- HAN L, XIAO T, TAN YZ, FANE AG and CHEW JW (2017) Contaminant rejection in the presence of humic acid by membrane distillation for surface water treatment. *J. Membrane Sci.* **541** (1) 291–299. <https://doi.org/10.1016/j.memsci.2017.07.013>
- HESTER J, BANERJEE P and MAYES A (1999) Preparation of protein-resistant surfaces on poly (vinylidene fluoride) membranes via surface segregation. *Macromolecules* **32** (5) 1643–1650. <https://doi.org/10.1021/ma980707u>
- HUANG S-H, LI C-L, HU C-C, TSAI H, LEE K-R and LAI J-Y (2006) Polyamide thin-film composite membranes prepared by interfacial polymerization for pervaporation separation. *Desalination* **200** (1–3) 387–389. <https://doi.org/10.1016/j.desal.2006.03.386>
- IDRIS A, ZAIN NM and NOORDIN M (2007) Synthesis, characterization and performance of asymmetric polyethersulfone (PES) ultrafiltration membranes with polyethylene glycol of different molecular weights as additives. *Desalination* **207** (1–3) 3244–339. <https://doi.org/10.1016/j.desal.2006.08.008>
- JAMES E (1999) *MARK, Polymer Data Handbook*. Oxford University Press, Inc., New York.
- KANG G-D and CAO Y-M (2012) Development of antifouling reverse osmosis membranes for water treatment: a review. *Water Res.* **46** (3) 584–600. <https://doi.org/10.1016/j.watres.2011.11.041>
- KANG G-D and CAO Y-M (2014) Application and modification of poly (vinylidene fluoride)(PVDF) membranes—A review. *J. Membrane Sci.* **463** 145–165. <https://doi.org/10.1016/j.memsci.2014.03.055>
- KIM JW, CHO WJ and HA CS (2002) Morphology, crystalline structure, and properties of poly (vinylidene fluoride)/silica hybrid composites. *J. Polymer Sci. Part B: Polymer Phys.* **40** (1) 19–30. <https://doi.org/10.1002/polb.10071>
- KIMMERLE K and STRATHMANN H (1990) Analysis of the structure-determining process of phase inversion membranes. *Desalination* **79** (2–3) 283–302. [https://doi.org/10.1016/0011-9164\(90\)85012-Y](https://doi.org/10.1016/0011-9164(90)85012-Y)
- LI J, LI M, MIAO J, WANG J, SHAO X and ZHANG Q (2012) Improved surface property of PVDF membrane with amphiphilic zwitterionic copolymer as membrane additive. *Appl. Surf. Sci.* **258** (17) 6398–6405. <https://doi.org/10.1016/j.apsusc.2012.03.049>
- LIU F, HASHIM NA, LIU Y, ABED MM and LI K (2011) Progress in the production and modification of PVDF membranes. *J. Membrane Sci.* **375** (1) 1–27. <https://doi.org/10.1016/j.memsci.2011.03.014>
- LOH CH and WANG R (2012) Effects of additives and coagulant temperature on fabrication of high performance PVDF/Pluronic F127 blend hollow fiber membranes via nonsolvent induced phase separation. *Chin. J. Chem. Eng.* **20** (1) 71–79. [https://doi.org/10.1016/S1004-9541\(12\)60365-6](https://doi.org/10.1016/S1004-9541(12)60365-6)
- MA Z, LU X, WU C, GAO Q, ZHAO L, ZHANG H and LIU Z (2017) Functional surface modification of PVDF membrane for chemical pulse cleaning. *J. Membrane Sci.* **524** 389–399. <https://doi.org/10.1016/j.memsci.2016.11.063>
- MAHLAMBI MM, VILAKATI GD and MAMBA BB (2014) Synthesis, characterization, and visible light degradation of rhodamine B dye by carbon-covered alumina supported Pd-TiO<sub>2</sub>/polysulfone membranes. *Sep. Sci. Technol.* **49** (14) 2124–2134. <https://doi.org/10.1016/j.memsci.2009.12.035>

1080/01496395.2014.917105

- MEYERS H and MYERS H (1997) *Introductory Solid State Physics*. CRC Press, Florida. <https://doi.org/10.4324/9780203212554>
- PADAKI M, ISLOOR AM, ISMAIL AF and ABDULLAH MS (2012) Synthesis, characterization and desalination study of novel PSAB and mPSAB blend membranes with polysulfone (PSf). *Desalination* **295** 35. <https://doi.org/10.1016/j.desal.2012.03.014>
- PETERSEN RJ and CADOTTE JE (1990) Thin film composite reverse osmosis membranes. In: Porter MC [ed.] *Handbook of Industrial Membrane Technology*. Noyes Publications, New Jersey. 307–343.
- PRADEEP GG, SUKUMARAN KP, GEORGE G, MUHAMMAD F and MATHEW N (2016) Production and characterization of activated carbon and its application in water purification. *Int. Res. J. Eng. Technol.* **2** (8) 443–447.
- RAHIMPOUR AM, MADAENI SS, GHORBANI S, SHOCKRAVI A and MANSOURPANAH Y (2010) The influence of sulfonated polyethersulfone (SPES) on surface nano-morphology and performance of polyethersulfone (PES) membrane. *Appl. Surf. Sci.* **256** 1825–1832. <https://doi.org/10.1016/j.apsusc.2009.10.014>
- RAJESH S, SENTHILKUMAR S, JAYALAKSHMI A, NIRMALA M, ISMAIL AF and MOHAN D (2013) Preparation and performance evaluation of poly (amide-imide) and TiO<sub>2</sub> nanoparticles impregnated polysulfone nanofiltration membranes in the removal of humic substances. *Colloids Surf. A: Physicochem. Eng. Aspects* **418** 92–104. <https://doi.org/10.1016/j.colsurfa.2012.11.029>
- RANA D and MATSUURA T (2010) Surface modifications for antifouling membranes. *Chem. Rev.* **110** (4) 2448–2471. <https://doi.org/10.1021/cr800208y>
- SALJOUGH I E and MOUSAVI SM (2012) Preparation and characterization of novel polysulfone nanofiltration membranes for removal of cadmium from contaminated water. *Sep. Purif. Technol.* **90** 22–30. <https://doi.org/10.1016/j.seppur.2012.02.008>
- SARRIA-VILLA R, OCAMPO-DUQUE W, PÁEZ M and SCHUHMACHER M (2016) Presence of PAHs in water and sediments of the Colombian Cauca River during heavy rain episodes, and implications for risk assessment. *Sci. Total Environ.* **540** 455–465. <https://doi.org/10.1016/j.scitotenv.2015.07.020>
- SHEN L, BIAN X, LU X, SHI L, LIU Z, CHEN L, HOU Z and FAN K (2012) Preparation and characterization of ZnO/polyethersulfone (PES) hybrid membranes. *Desalination* **293** 21–29. <https://doi.org/10.1016/j.desal.2012.02.019>
- SHEN L, FENG S, LI J, CHEN J, LI F, LIN H and YU G (2017) Surface modification of polyvinylidene fluoride (PVDF) membrane via radiation grafting: novel mechanisms underlying the interesting enhanced membrane performance. *Sci. Rep.* **7** (1) 2721. <https://doi.org/10.1038/s41598-017-02605-3>
- VATANPOUR V, MADAENI SS, MORADIAN R, ZINADINI S and ASTINCHAP B (2012) Novel antibifouling nanofiltration polyethersulfone membrane fabricated from embedding TiO<sub>2</sub> coated multiwalled carbon nanotubes. *Sep. Purif. Technol.* **90** 69–82. <https://doi.org/10.1016/j.seppur.2012.02.014>
- WANG Y, GOH SH, CHUNG TS and NA P (2009) Polyamide-imide/polyetherimide dual-layer hollow fiber membranes for pervaporation dehydration of C1–C4 alcohols. *J. Membrane Sci.* **326** (1) 222–233. <https://doi.org/10.1016/j.memsci.2008.10.005>
- YAN L, LI YS and XIANG CB (2005) Preparation of poly (vinylidene fluoride)(pvdF) ultrafiltration membrane modified by nano-sized alumina (Al<sub>2</sub>O<sub>3</sub>) and its antifouling research. *Polymer* **46** (18) 7701–7706. <https://doi.org/10.1016/j.polymer.2005.05.155>
- YANG Y, ZHANG H, WANG P, ZHENG Q and LI J (2007) The influence of nano-sized TiO<sub>2</sub> fillers on the morphologies and properties of PSF UF membrane. *J. Membrane Sci.* **288** (231) 1–2. <https://doi.org/10.1016/j.memsci.2006.11.019>
- ZELEDON-TORUNO ZC, LAO-LUQUE C, DE LAS HERAS FXC and SOLE-SARDANS M (2007) Removal of PAHs from water using an immature coal (leonardite). *Chemosphere* **67** (3) 505–512. <https://doi.org/10.1016/j.chemosphere.2006.09.047>
- ZHANG Y, ZHONG S, ZHANG M and LIN Y (2009) Antibacterial activity of silver-loaded zeolite A prepared by a fast microwave-loading method. *J. Mater. Sci.* **44** (2) 457–462. <https://doi.org/10.1007/s10853-008-3129-5>
- ZHU Y, WANG D, JIANG L and JIN J (2014) Recent progress in developing advanced membranes for emulsified oil/water separation. *NPG Asia Mater.* **6** (5) e101. <https://doi.org/10.1038/am.2014.23>